PCCP

ROYAL SOCIETY OF CHEMISTRY

PAPER

View Article Online
View Journal

Cite this: DOI: 10.1039/d5cp03690a

pH-dependent peptide aggregation and translocation across octanol and hexane interfaces: insights from umbrella sampling simulations

Anjana V. Mathath, Samrat Sarkar and Debashree Chakraborty *

The pH-dependent peptides are membrane-permeabilizing peptides that can form macromolecular-sized pores at an acidic pH. Their mode of aggregation and mechanism of action with the cell membrane are still elusive. Herein, we approach the study of the aggregation and translocation pathways of pHD24 peptides through octanol–water and hexane–water interfaces at an acidic pH (pH 4) and a physiological pH (pH 7) to identify the differences in activities. The octanol–water interface and the hexane–water interface are known to mimic the complex phospholipid bilayers and are suitable as simple models for studying the multiple-peptide actions. At the acidic pH, the pHD24 peptides are found to be aggregated and translocated across the interface more easily than at pH 7. At the octanol–water interface, the peptides are translocated through a narrow water channel with an energy barrier of 309.6 kJ mol^{-1}. The favourable peptide–peptide interaction, facilitated by hydrogen bonding and electrostatic interactions, enhances peptide aggregation at pH 4 and contributes to the formation of a relatively large pore. The results are in good agreement with the translocation of the pHD24 peptides through the heterogeneous membrane at an acidic pH. This study provides insights into the aggregation and translocation abilities of pHD peptides at a low pH through biomembrane mimic model systems, shedding light on the design of strategies for synthetic peptides in drug delivery.

Received 24th September 2025,
Accepted 24th November 2025

DOI: 10.1039/d5cp03690a

rsc.li/pccp

1. Introduction

Membrane-active peptides that are sensitive to changes in pH can be used to transport molecules into cells through endosomes.[1,2] This makes them useful in drug delivery and other medical applications, particularly for targeting cancer[3–5] cells. The mechanism of action of pH-dependent delivery (pHD) peptides involves inducing pH-sensitive properties in the peptide, which allow it to interact with the membrane at a specific pH. These peptides are able to trigger the leakage of large molecules through a synthetic membrane under acidic (pH $\leq$ 6) conditions.[6,7] The peptide undergoes membrane insertion and folding in response to changes in pH, allowing it to deliver cargo to cells in acidic environments.

The evolution of pHD peptides comes from melittin, as the parent peptide. Later, a derivative of melittin is produced, which is MelP5, a potent peptide that can form a macromolecular-sized pore at high concentrations and across all pH.[8] However, the pHD peptides can only induce the release of macromolecules at an acidic pH and even at a low peptide concentration. At pH 7 or above, these peptides are essentially inactive and do not release small or large molecules from lipid bilayer vesicles. All the available pHD peptides have mostly five acidic residues, and the largely studied peptides are pHD15, pHD24, and pHD108.[6,7,9] The insertion and folding of proteins into a membrane is a complex process, and an atomistic-level description of this process remains poorly understood. In this regard, MD simulation can act as an important tool to gain insight for a proper understanding of the passive permeation and its energetics. Theoretically, it has been reported that pHD108 can form a macromolecular-sized pore by vesicle formation at an acidic pH.[10]

The atomistic detail study of the folding and aggregation of the peptides in the membrane environment is a costly process. The process of aggregation involves the diffusion of the peptides from randomly oriented conformations on the interface surface, which is a slow process compared with the timescale of the MD simulations due to the slow relaxation of the collective motion of the lipid molecules in the bilayer. Generally, long-term sampling is required to form the probable secondary structure of peptides in the aggregated state on the membrane surface. This can be easily achieved with the alkane/alkanol–water interface systems. Furthermore, incorporating the peptides into the lipids will involve the spatial rearrangements of

Biophysical and Computational Chemistry Laboratory, Department of Chemistry, National Institute of Technology Karnataka, Surathkal, Mangalore, 575 025, Karnataka, India. E-mail: debashree@nitk.edu.in

the lipid molecules. In this respect, the water–hexane and water–octanol interfaces can help in mimicking a system similar to the cell membrane to study the insertion pathway of the peptide aggregates at different pH values. It is well known that the octanol–water interface can act as an alternative to phospholipids, which consist of a lipid bilayer. Because of this reason, the quantity of lipophilicity is generally expressed in terms of the water/octanol partition coefficient. Similarly, there are some studies with the hexane–water system, and it is also reported to mimic the cell environment.[11] Both these interface systems are close to the water-membrane system, where the difference between the aqueous and non-aqueous phases with varied dielectric constants can be mimicked. The interface between the two phases provides a consistent and reliable surface for the self-assembly of a diverse array of potential drug molecules. The interfacial system can contribute to the understanding of the interactions between the polar and nonpolar residues.[12] The carefully interpreted results of these interactions can be beneficial for understanding cellular processes.

This is particularly advantageous for those solutes that possess solubility in water and the ability to permeate through cellular membranes.[13] Hence, here, we consider both the hexane–water and octanol–water interfaces to study the factors affecting the permeation process of the pH-triggered peptide. This will help to reduce the computational cost of modeling the large lipid bilayer systems. Further, the results are compared with those of a heterogeneous membrane. There are some basic queries that remain to be answered to understand the proper functioning of the membrane-active peptides, such as what are the factors that affect the aggregation process in the membrane environment? Do peptides aggregate in more than one way? The aggregation of the peptides is considered to be one of the crucial steps for the permeation mechanism.[14] It has been proposed that around four peptides are critically required to form a pore. Since the permeation of one peptide is energetically more favourable than the permeation by four peptides at a time, does the permeation process initiated by a single peptide and the deformation experienced by the membrane environment further help in the permeation of the other peptides? There are reports stating that the cationic antimicrobial peptides prefer to be in a monomeric state in the solution and on the membrane surface.[15] On the other hand, peptides like melittin and Aβ(1-42) prefer to permeate in an aggregated fashion.[16,17] Therefore, this process totally depends on the type of peptide and the membrane environment. The process of the multimerization of the peptide actually depends on the peptide sequence and the lipid composition. The so-called 'soft membrane adapt and respond, also transiently' (SMART) model[18] is also proposed based on this notion.

In this article, we will concentrate on the pH-dependent peptide, pHD24, to find out the ways by which they prefer to stay on the membrane interface and translocate. The pHD24 is amphiphilic and has five acidic residues, which can induce substantial macromolecular leakage, more potent and optimal for the pH-triggered activity than peptides with six acidic residues, such as pHD15.[19] In order to gain insight into the peptide translocation processes, the common practice is to study the model peptides that permeate into membranes and remain in helical conformation in the bilayer environment.[7,8] However, the secondary structure and the permeability tendency of the peptide will largely vary from peptide-to-peptide case, and it will also depend on the peptide–lipid interaction. The aggregation of the peptides has been studied by coarse-grain simulations, as these processes are very slow compared with the time-scale of atomistic MD simulations.[20] In coarse-grain simulations, the systems are mainly studied at a neutral pH; therefore, the effectiveness of these peptides according to pH cannot be studied.

Recent studies regarding the coarse-grain simulation carried out by incorporating pH-sensitive dummy beads are appreciable.[21] However, this cannot be utilized for studying multiple peptide insertions through membrane-mimicking systems or model lipid bilayers. These coarse-grain models lack the explicit representation of hydrogen bonding, side-chain interactions, and dielectric effects under acidic conditions. Therefore, atomistic simulations are essential for capturing how a change in the protonation state affects peptide conformation and peptide–peptide, peptide–lipid, and peptide–water interactions to understand the permeation pathways.

One of the major factors that can significantly alter the behavior of these peptides is the pH of the medium. This is because the charge on the side chains which is dependent on the pH of the surrounding environment.[22] The protonation state of amino acid side chains changes at different pH levels, which results in differences in the charges.[23] The pH-dependent conformational changes in proteins are influenced mainly by three primary factors: interactions between the peptide charges with the solvent molecules and the lipid head groups, inter-peptide interactions, and the effect of dehydration, also known as the Born effect,[24,25] when the peptide permeates the membrane. As mentioned above, the activities of the pHD peptides are very much dependent on the effect of pH; therefore, a thorough study is required in this respect to investigate the response of these peptides to the different membrane-like systems. Experimentally and theoretically, there are few studies regarding the investigation of the pH effect on the aggregation of peptides.[26,27] In view of this, here, we aim to study the aggregation propensity and structural details of the pH-dependent peptides at the octanol–water and hexane–water interfaces, varying the pH values (acidic pH: 4 and neutral pH: 7), by atomistic MD simulations. Even though some experimental studies[6,7,9] have been done for these peptides, theoretical studies are very rare.

We employ two different force fields, CHARMM and AMBER, for the peptides for comparison. Further, we calculate the free energy of translocation by the umbrella sampling techniques to obtain an overview of the permeation mechanism. The present work explicitly addresses the process of self-aggregation and the different modes of the translocation process across the interface by treating it in full atomistic detail. In the following section, we describe the methodology, followed by the results and discussion.

2. Methodology

2.1. System preparation and simulation details

All-atom simulations were performed to study the structural changes, aggregation, and translocation of the peptides through the octanol–water and hexane–water interfaces at two different pH levels, pH 4 and pH 7, in two force fields, amber99sb-ILDN[28] and CHARMM36m,[29] using GROMACS[30] software. The initial structures were created using the Packmol package.[31] The compositions of all the simulated systems are detailed in Table 1.

2.1.1. Preparation of the interface. We prepared the interface systems by creating a normal bulk hexane/octanol system with a box dimension of 8.5 nm × 8.5 nm × 6.5 nm (the x, y, and z directions, respectively). The energy of the initial structure was minimized using the steepest descent algorithm. The systems were equilibrated in the canonical ensemble (NVT) and then in the isothermal–isobaric ensemble (NPT) for 10 ns and 20 ns, respectively. Subsequently, a 20-ns production run was performed, resulting in the system becoming equally dense in all directions. After that, we extended the length of the Z direction of the box to 13 nm. The area excluding the hexane/octanol molecules in the entire box was solvated with TIP4P[32] water molecules. Then, peptides were introduced into the interface.

2.1.2. Preparation of the peptides. Peptide pHD24 (GIGDVLHELAADLPELQEWIHAAQQL) was initially constructed as a random coil using Avogadro software.[33] During the 1 μs simulation, it transitioned through different secondary structures. At a neutral pH, the peptide carried a charge of −5, while at pH 4, it carried a charge of −3. To neutralise the systems, we added Na^+ ions. The pKa values for the side chains of the histidine (H) residue, aspartic acid (D) residue, and glutamic acid (E) residue were 6.04, 2.87, and 3.08, respectively. In general, if the pH value is lower than the pKa value, the protonation of the side chain must occur. Hence, at an acidic pH of 4, two histidine groups (residues 7 and 21) must be protonated.

2.1.3. Introduction of the peptides on the interface. Four peptide molecules were randomly distributed throughout the simulation box (two in the hexane/octanol part for the interface systems and two in the water part) to avoid any potential biased effects on the self-assembly process. Energy minimization had to be performed using the steepest descent algorithm. The systems were equilibrated in NVT and then NPT for 10 ns and 50 ns, respectively, with the solute-heavy atoms restrained. Subsequently, the restraints were removed, and the protein molecules were allowed to move freely during the 1-μs production run, with a frame saved every 10 ps to collect the simulation trajectory.

The semi-isotropic Berendsen algorithm[34] was applied for the interface systems to couple the pressure in the Z dimension (reference pressure (P_Z) of 1 bar, compressibility of 4.5×10^{-5} bar^{-1}, and relaxation time of 3 ps) while keeping the XY plane fixed with a compressibility of zero. Three-dimensional periodic boundary conditions (PBC) were used. Short-range Coulomb interactions were calculated up to 1.2 nm, with long-range interactions calculated using the particle mesh Ewald (PME) method.[35] Short-range van der Waals (vdW) interactions using the Lennard-Jones 12-6 potential were calculated up to 1.2 nm, along with long-range dispersion correction for energy and pressure. All chemical covalent bonds were constrained using the LINCS algorithm,[36] supporting a leapfrog integration time of 2 fs.

The trajectories were visualized using the VMD software.[37] Furthermore, US simulations were conducted, and the details regarding RC, free energy calculation, and convergence are provided in the following sections. We performed two independent replicas of 1 μs unbiased MD simulations for four pHD24 peptides in the octanol–water and hexane–water interface systems. The last 100 ns trajectory was used for the analysis. The pressure convergence plots corresponding to each equilibrated system are shown in the SI, Fig. S1. The convergence analysis confirmed that two trajectories should be statistically adequate for excellent convergence. We have given the result of the AMBER force field in the manuscript and shown the results corresponding to the CHARMM force field in the SI. The results of the CHARMM force field are discussed wherever applicable.

2.1.4. Preparation and simulation details of the lipid bilayer-peptide systems. We built the heterogeneous symmetric lipid bilayer composed of 1-palmitoyl-2-oleoyl-phosphatidylcholine (POPC), 1-palmitoyl-2-oleoyl-phosphatidylserine (POPS), and cholesterol (CHOL) molecules in a ratio of 7:2:1 using CHARMM-GUI[38] software. We simulated a total of two systems, as the four pHD24 peptides randomly adsorbed on the membrane upper hydrophilic–hydrophobic interface at pH 4 and pH 7. We added NaCl to neutralize the system. The details of the system setup are tabulated in Table 2.

All MD simulations were performed using GROMACS 2022.2 software.[39] The CHARMM36 force field[40] with a correction map (cmap) was used to parameterize the lipid molecules, and CHARMM36m[41] was used to parameterize the peptides. The membrane–peptide systems were solvated with the TIP3P water model.[42] Energy minimization was performed using the steepest descent algorithm to remove steric clashes between the lipid and lipid–water molecules. The PME algorithm[35] was used to compute the long-range electrostatic interactions, and van der Waals interactions were computed with a cutoff of 1.2 nm. The hydrogen bonds were restrained using the LINCS algorithm.[36] The system temperature was maintained at 300.15 K using the v-rescale temperature coupling algorithm

Table 1 Compositions and dimensions of the simulated interface systems

Systems	Systems	pH	No. of hexanes/octanols	No. of waters	No. of peptides	L_{XY} (nm)	L_Z (nm)
System 1	Hexane–water	4	2406	16597	4	9	13
System 2	Hexane–water	7	2406	16616	4	9	13
System 3	Octanol–Water	4	1952	19532	4	9	13
System 4	Octanol–Water	7	1952	19548	4	9	13

Table 2 Detailed information regarding the heterogeneous, symmetric membrane peptide (pep) systems at pH 4 and 7

Systems	Pep	POPC	POPS	CHOL	Water	Na^+	Cl^-
Memb-pep (pH 4)	4	140	40	20	12574	64	12
Memb-pep (pH 7)	4	140	40	20	12615	73	13

with a time constant of 1 ps (τ_T = 1 ps) in the NVT ensemble. Then, the systems were equilibrated in the NPT ensemble to achieve the desired density. The Parrinello–Rahman[43] semi-isotropic pressure coupling was used to maintain the pressure of 1 bar with a time constant (τ_P) of 5 ps and compressibility of 4.5×10^{-5}/bar. Each system was well equilibrated for ~45 ns. Then, the production run was carried out for up to 350 ns.

2.2. Umbrella sampling (US) simulations

The free energy barrier was computed to translocate the multiple pHD24 peptides through the water-organic interface using the umbrella sampling[44] (US) method. Here, the reaction coordinate (RC) employed for the US simulations was defined as the *Z*-coordinate distance between the center of mass of all peptides (as a single group) and the center of mass of the reference system.

$$\xi = Z_{pep} - Z_{com} \quad (1)$$

We have performed the US simulations for the four pHD24 peptides in the octanol–water and hexane–water systems simulated in the amber99sb-ILDN force field. For each system, all peptides were pulled at a rate of 0.005 nm ps^{-1} and a force constant of the bias potential of 500 kJ mol^{-1} nm^{-2}.

For the membrane–peptide system, we pulled all the peptides at a rate of 0.005 nm ps^{-1} with a force constant of the bias potential of 100 kJ mol^{-1} nm^{-2}. In this case, the RC applied was the *Z*-coordinate distance between the center of mass of all peptides (as a single group) and the center of mass of the membrane.

Later, the weighted histogram analysis method (WHAM)[45] was used to construct potential of mean force (PMF) profiles and estimate statistical errors. We pulled four peptides from the water–organic (hexane and octanol) interface towards the organic medium. This was performed for systems at pH 4 (acidic pH) and neutral pH 7 (physiological pH). Similarly, all the peptides were pulled from the membrane hydrophilic–hydrophobic interface through the hydrophobic core of the membrane towards the aqueous region. A window spacing of 0.2 nm was used to collect the initial windows for the US simulation. In the case of the octanol–water and hexane–water systems, ~28 windows were sampled. For the membrane–peptide systems, around 42 windows were simulated for 5 ns of equilibration, followed by 50 ns of production sampling. The window simulations were replicated twice and found to converge around 45 ns, which was then extended to 50 ns; the convergence plots are shown in Fig. S2.

3. Results and discussion

In the following sections, we discuss the aggregation tendency, translocation pathways, and free energy barrier of four pHD24 peptides through the octanol–water and hexane–water interfaces at pH 4 and 7. All the results discussed here are those for the AMBER force field. In the CHARMM force field, the results followed a similar trend, and their corresponding data are provided in the SI. Later, we compared our results to those of the heterogeneous symmetric membrane–peptide systems at both pH levels.

3.1. Aggregation of pHD24 in the interfaces

In both interface systems, peptides were found to reside at the interface between the water and organic layers. The aggregation tendencies of the pHD24 peptides in both the octanol–water and hexane–water interfaces at the acidic pH and neutral pH in the AMBER force field are shown in Fig. 1.

In the case of the octanol–water medium, the peptides had a more elongated and extended structure as compared with peptides in the hexane–water interface. The compactness of the peptides can be found from the probability density curve of the radius of gyration (R_g) data given in Fig. 2a. Here, the maximum probability density of R_g for the hexane–water

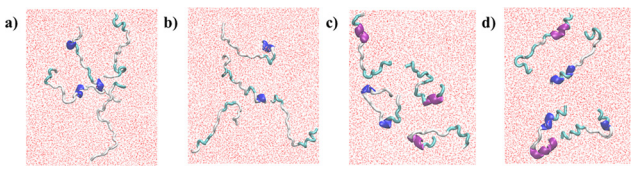

Fig. 1 Snapshot of the aggregate of the pHD24 peptide formed at the (a) octanol–water interface at pH 4, (b) octanol–water interface at pH 7, (c) hexane–water interface at pH 4, and (d) hexane–water interface at pH 7 in the AMBER force field.

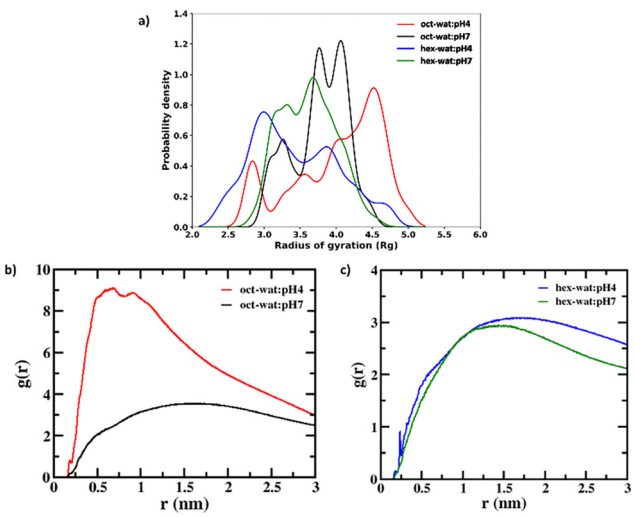

Fig. 2 (a) Probability density of the radius of gyration (nm) of the peptides; peptide–peptide RDF plots at the interface for (b) octanol–water at pH 4 (red) and pH 7 (black) and (c) hexane–water at pH 4 (blue) and pH 7 (green) in the AMBER force field.

Table 3 The maximum number of hydrogen bonds for the inter-peptide, intra-peptide, and peptide–water cases in the octanol–water and hexane–water systems when the peptides are in the interface at pH 4 and pH 7 in the AMBER force field

	Octanol–water		Hexane–water	
Pairs	pH 4	pH 7	pH 4	pH 7
Peptide–peptide (inter)	10	2	4	2
Peptide–peptide (intra)	24	30	41	40
Peptide–water	302	311	311	318

system was shifted towards a relatively low R_g value, while for the octanol–water system, it was shifted to a relatively high R_g value. In the case of the octanol–water system, the maximum probability density of R_g value was ~4.6 nm at pH 4 and ~4.1 nm at pH 7 (Fig. 2a). This confirmed the extended structure of the peptides at the octanol–water interface at pH 4 (Fig. 1a). In Fig. 2b and c, we have plotted the radial distribution function of the center of mass of one peptide with respect to the center of mass of the other three peptides in the interface. It was evident that at pH 4, for the octanol–water interface, the peptides had the maximum aggregation tendency as compared with other systems.

Hence, we found the maximum probability of the peptide–peptide interaction at pH 4 than at pH 7 in this case (Fig. 2b). At pH 7, the peptides were found to be nearby without any direct linkage. The probability density of R_g data in the case of the CHARMM force field is given in the SI, Fig. S3. For the hexane–water system, the peptides were found to be compact and rigid with a maximum probability of R_g value of ~3.0 nm and ~3.7 nm at pH 4 and pH 7, respectively. The four peptides were found to be near each other, yet no direct linkage was observed at pH 4 (Fig. 1c). While at pH 7, two peptides were found to come near each other as a dimer (Fig. 1d). The hydrogen bonds formed between the peptides and peptide with water in the AMBER force field and the CHARMM force field are given in Table 3 and Table S1, respectively.

In general, the peptide–peptide aggregation is facilitated by the inter-peptide–peptide hydrogen bond and electrostatic interactions. In our study, at pH 4, the peptides tend to aggregate more, with favourable inter-peptide hydrogen bond interactions, than at pH 7.

In the octanol–water interface, the peptides were found to be interconnected more at pH 4 due to the relatively high number of inter-peptide–peptide interactions (around 10), with an electrostatic attractive interaction of −38627 kJ mol^{-1}. The Coulombic interaction energy data between the peptides when they are in the interface in the CHARMM force field are provided in Table S2. Because of the high number of interpeptide interactions, the intra-peptide hydrogen bond interaction and interaction with the water molecules were comparatively fewer at pH 4 than at pH 7. Hence, the peptides were favourably aggregated in the octanol–water interface at pH 4. While at pH 7, the peptides were found to be near each other without any direct linkage, with the least Coulombic interaction of −37571 kJ mol^{-1}.

At the acidic pH, the peptides formed additional hydrogen bonds due to the protonation state of the histidine residues and had more hydrogen bonds between the peptides and fewer hydrogen bonds with water than at pH 7. In our case, we found the interaction of protonated histidine (HIP21) in one peptide chain with the GLN24 residue of another peptide and HIP7 residue in one peptide with the ALA23 residue in another peptide chain at pH 4 in the octanol–water interface, which facilitated the aggregation (Fig. S4). The solvent environment, pH, and the presence of interfaces influenced the variations in the peptide–peptide interactions in the different systems.

The numbers of inter-peptide hydrogen bonds formed in the hexane–water case at pH 4 and pH 7 were around 4 and 2, respectively, which were lower than those for the octanol–water system. However, this interface had a relatively large number of intra-peptide hydrogen bonds. We computed the secondary structures of the peptides using the DSSP algorithm, which are tabulated in Table 4, and the plots are given in Fig. S5 for the AMBER force field. Similarly, the secondary structure data of the peptides in the CHARMM force field were obtained and are presented in Table S3. At the interfaces, the peptides could interact with both hydrophobic and hydrophilic environments. This balance affected the secondary structures. A higher percentage of the secondary structures was observed for the peptide in the hexane–water interface systems than for the peptide in the octanol–water interface.

This was because the octanol was more amphiphilic in nature, and it interacts with the peptides, which reduces the percentage of the secondary structure of the peptides compared to that of the hexane–water system. In other words, hexane's nonpolar nature restricted its interaction with peptides, resulting in minimal hydrophobic interactions. Consequently, the peptides interacted more with themselves/each other, leading to a more compact protein structure, as indicated by the increased intramolecular hydrogen bonds.

The intra-peptide bond affected the secondary structure of the peptides. At pH 4, a relatively high percentage of extended random coil structures (61%) was observed for the octanol–water interface, which could be related to the high probable R_g value (Fig. 2a). The peptides also showed the beta-sheet formation tendency only at pH 4 (2% beta sheet and 2% beta bridge).

Table 4 Percentage of the secondary structures of the peptides for the octanol–water and hexane–water systems at pH 4 and 7 in the AMBER force field

Interface systems	pH	Total % of structured/ordered	A-helix	3-helix	β sheet	β bridge	Coil	Bend	Turn
Octanol–water	4	18	2	6	2	2	61	13	13
	7	24	6	9	0	0	52	12	17
Hexane–water	4	34	18	13	2	1	42	9	14
	7	28	13	13	0	0	44	12	16

In the case of the hexane–water system, the strong intra-peptide hydrogen bonds discussed above (Table 3) gave rise to a higher percentage of secondary structure content (sum of the percentages of alpha helix, beta-sheet, beta-bridge, and turn content) than in the octanol–water system. Further, the total percentage of the structured content of the peptide was found to be high at pH 4, in contrast to the trend seen in the octanol–water case. More alpha helix content was observed at pH 4 (18%) than at pH 7 (13%) in this case. At pH 4 and 7, the peptide–peptide coulombic interaction energies were −38683 kJ mol^{-1} and −38143 kJ mol^{-1}, respectively.

Therefore, in our study, we found that the hexane–water interface stabilizes the peptides with a favourable intra-peptide interaction. While the octanol–water interface served as a suitable amphiphilic hydrophobic environment, it facilitates contact with other peptides, leading to aggregation and suitable interpeptide interactions. The peptides at the octanol interface had a more extended structure and less percentage of secondary structures. The aggregation tendency was found to occur more at a low pH due to the protonation state of the histidine residue. The aggregation tendency of the pHD24 peptides in the interface and their interaction with the water and organic layers affected their translocation across the organic layer, and hence, in the next section, we explore the translocation pathway of the four pHD24 peptides through the octanol–water and hexane–water media at acidic and neutral pH.

3.2. Translocation of the pHD24 aggregate through the octanol–water interface

In this section, we discussed the aggregation and translocation of four pHD24 peptides through the octanol–water interface at pH 4 and pH 7 in the AMBER force field. We used the AMBER trajectory since the peptides were found to be significantly aggregated in this force field. The translocation pathway for the octanol–water system is given in Fig. 3.

Initially, the four pHD24 peptides were found to be arranged randomly over the octanol–water interface in a planar manner. As we have already seen in the previous section, due to the enhanced inter-peptide interactions, the four pHD24 peptides were found to be more aggregated and compact at pH 4; during translocation, they maintained that trend. Here, all peptides were found to be translocated together, which confirmed their cooperative activity during the permeation. This was further confirmed from the interaction energy data of the four pHD24 peptides during the permeation across the octanol and hexane media from the interface (Table 5).

As shown in Table 5, the peptide–peptide interaction is more prominent at a low pH than at pH 7 during the translocation. The peptides were found to have more interaction with water than the organic layer at both pH levels. For the hexane–water interface, this interaction was found to be more. Hence, when the peptides permeated, they carried water with them during the translocation. In the octanol–water interface at pH 4, the peptides were translocated through the octanol phase from the interface by creating a pore with a narrow water channel, which partitioned the octanol layer into two phases (Fig. 3d–f). The low aggregation propensity and strong peptide–octanol interaction at pH 7, however, did not result in a well-defined water channel, as shown in Fig. 3j. The water density across the octanol medium during the peptide translocation was higher at pH 4 than at pH 7, as shown in Fig. 4, which further confirmed the formation of a large pore, allowing the permeation of water molecules at a low pH.

At pH 7, the peptides were found to diffuse through the octanol phase; no well-defined pore was created (Fig. 3j–l). The peptides took some water with them during the permeation, and hence, we found the leakage of water. The free energy barrier for the translocation of peptides is shown in Fig. 6. It can be seen that the free energy barrier at pH 4 was lower compared to that at pH 7. The translocation barrier for the four pHD24 peptides to cross through the octanol medium was 309.6 kJ mol^{-1} at pH 4 and 686.7 kJ mol^{-1} at pH 7. The formation of a big pore and a low free energy barrier can be explained by the cooperative activity of the peptides at pH 4. The aggregation of the peptides at this pH helped the smooth permeation of all four peptides. Next, we discussed the permeation pathway of the peptides across the hexane–water interface.

3.3. Translocation of the pHD24 aggregate through the hexane–water interface

In Fig. 5, the translocation pathways of the four pHD24 peptides through the hexane–water interface are given at pH 4 and pH 7. In the case of the hexane–water interface, the peptides were compact, but they were not interlinked. They had more intra-peptide hydrogen bonds that helped them to maintain their secondary structures.

At pH 4, the peptide conformations were found to be more compact (Fig. 5b–d) than those at pH 7. Even though the hexane medium was hydrophobic in nature, the peptides suffered repulsive interactions with the medium, and the interaction energy of peptide–hexane was 3.92 kJ mol^{-1}. The peptides had a tendency to interact with the water molecules, and hence, during translocation, they proceeded with some water molecules through the hexane medium. We found that water leakage was created during the translocation of the four pHD24 peptides (Fig. 4). However, the water density here was lower compared to that in the octanol system. This was due to the repulsion of the hexane molecules with the water, and hence, the density was quite low. Octanol had a strong attractive interaction with the water molecules at both pH levels.

At pH 7, (Fig. 5e–h) the peptides had a slight attractive interaction, around −0.92 kJ mol^{-1}, with the hexane medium and a strong attractive interaction with the water molecules, which helped to translocate easily through the water channel in comparison to those at pH 4 (Fig. 5a–d). The water density in the pore was found to be high at pH 7 for the hexane–water system (Fig. 4). The differences in the permeation pathways, as understood from the PMF profile computed from the US simulations, are plotted in Fig. 6.

The four pHD24 peptides faced a higher energy barrier during the permeation through the hexane medium compared to the barrier for the octanol medium. At pH 7, as discussed above, due to a favourable interaction with the organic layer

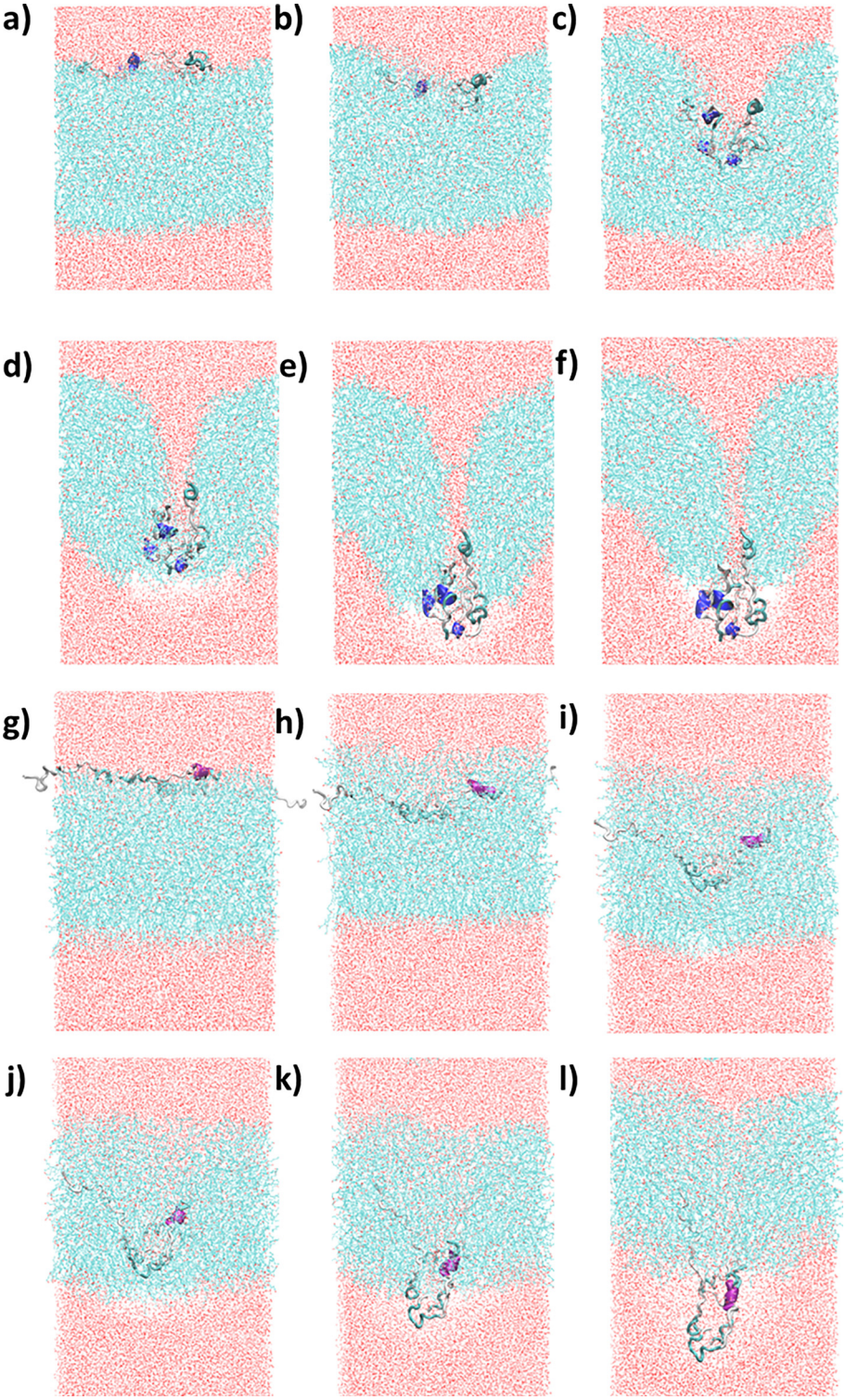

Fig. 3 US simulation snapshots of the translocation pathways of the four pHD24 peptides through the octanol–water interface at (a)–(f) pH 4 and (g)–(l) pH 7 in the AMBER force field. The periodic boundary condition is applied for water molecules in the $-Z$ direction to clearly represent the image.

(Table 5) in comparison to that at pH 4, the translocation of the peptides was easy. Hence, the free energy barrier of the translocation of the four pHD24 peptides through the hexane medium was lower at pH 7 (such as 1016.4 kJ mol^{-1}) than at pH 4 (1321.3 kJ mol^{-1}), as shown in Fig. 6b. That is, the cooperative action of the four peptides helped to permeate multiple peptides at pH 7 through the hexane medium, which reduced the energy barrier.

In the CHARMM36m force field, the peptides were found to be more elongated and extended at the octanol–water interface,

Table 5 The Coulombic interaction energy (IE) between peptide–peptide, peptide–organic layer (octanol/hexane), peptide–water, and organic layer-water during the four pHD24 translocations across the octanol–water and hexane–water interface systems at pH 4 and pH 7 in the AMBER force field

	IE in the octanol–water system (kJ mol^{-1})		IE in the hexane–water system (kJ mol^{-1})	
Pairs	pH 4	pH 7	pH 4	pH 7
Peptide–peptide	−37325	−35812.4	−37098.4	−36358.6
Peptide–organic	−1310.53	−1774.33	3.92111	−0.921339
Peptide–water	−12178.3	−12127.6	−14611.2	−14670.2
Organic–water	−30784.9	−30595.8	109.786	113.181

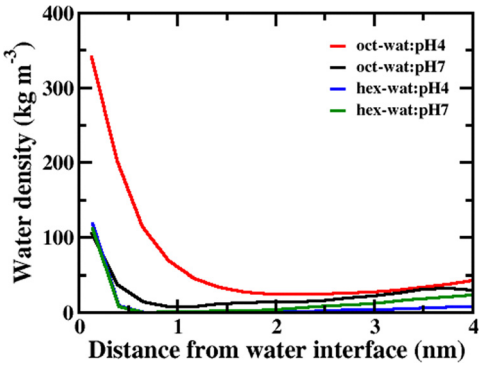

Fig. 4 The water density along the distance from the water interface (nm) during the translocation of the peptides across the octanol and hexane media at both pH levels.

similar to those in the AMBER force field. At pH 4, the peptides were likely to be aggregated and translocated through the octanol medium with some water leakage. However, for pH 7, the peptide aggregate was found to be stuck inside the octanol medium (Fig. S6). At the hexane–water interface, the peptides were found to be well-aggregated and compact. However, they faced a barrier to permeating completely through the hexane medium, so that the peptides were found to be trapped inside at both pH 4 and pH 7 (Fig. S7), similar to the results presented in Fig. 5.

Our octanol–water system was found to accurately depict the experimental findings of Kim *et al.*,[6] which indicated that synthetic pHD24 peptides could aggregate and permeate across the hydrophobic medium, forming a macromolecular-sized pore of a water channel at an acidic pH. The hexane–water system clearly showed that when the number of peptide–membrane interactions was low, the peptide faced a relatively high energy barrier during permeation.

3.4. Confined water dynamics during peptide translocation

As we discussed in the earlier sections, the peptide translocation through the octanol and hexane medium was facilitated by the formation of a water channel. The dynamics of the confined water during the peptide translocation were understood by computing the hydrogen bond lifetime[46] (HBL) and diffusion coefficient[47] (D_c) given in Table 6. Generally, two water molecules were said to be hydrogen bonded when the H···O distance is less than 2.5 Å and the O–H···O angle is less than 130°. The expression used to calculate the hydrogen bond lifetime from the hydrogen bond population operator is given as follows:

$$S_{HB}(t) = \frac{\langle h(0) \cdot H(t) \rangle}{\langle h(0)^2 \rangle}. \quad (2)$$

Here, $H(t)$ is the population parameter, which is equal to 1 if the hydrogen bond exists or zero otherwise.[48]

We considered the water molecules around all the peptides within the range of 10 Å as the confined water molecules, as seen in the snapshot presented in Fig. 3d and j, 5d and h. Hydrogen-bond lifetime was found to be longer for the hexane–water systems at both pH levels than in the octanol–water case. This was because of the presence of more dispersed water around the peptides during their permeation. The high water density (Fig. 4) of the pore created in the case of the octanol–water system during peptide permeation increased the cooperative action of the hydrogen bond making and breaking, leading to a shorter hydrogen bond lifetime than the hexane–water interface system.

At pH 4, in the octanol–water interface system, water molecules were confined, forming a nanopore, compared to that at pH 7, resulting in a strong hydrogen bond and a long hydrogen bond lifetime (Fig. 3f). On the contrary, water molecules were more dispersed as monomers around the peptides at pH 7, resulting in comparably weak hydrogen bonds and short hydrogen bond lifetimes (Fig. 3k).

We also calculated the diffusion coefficient of confined and bulk water during the peptide translocation in the interface systems. The self-diffusion coefficient value of water, computed experimentally by J. H. Simpson and HY. Carr,[49] is 2.13 × 10^{-5} cm^2 s^{-1}. Theoretically, D.V. Zlenko computed the diffusion coefficient of TIP4P water[50] at 298 K as ∼2.5 × 10^{-5} cm^2 s^{-1}. In our case, we obtained a self-diffusion coefficient value of 2.49 × 10^{-5} cm^2 s^{-1} for the bulk TIP4P water in the interface systems. It has been experimentally reported that the diffusion coefficient of the water molecules in *n*-octanol is less than that in the *n*-hexane medium.[51] This is due to the hydrogen bonding and electrostatic interactions of the water molecules with the hydroxyl group of octanol, which slow down the diffusion of water. In our case, water molecules were found to be more diffusive in the hexane–water system at both pH levels than in the octanol–water system. The nanoconfined water in the octanol–water interface at pH 4 had the lowest diffusion coefficient. The behavior of the confined water around the

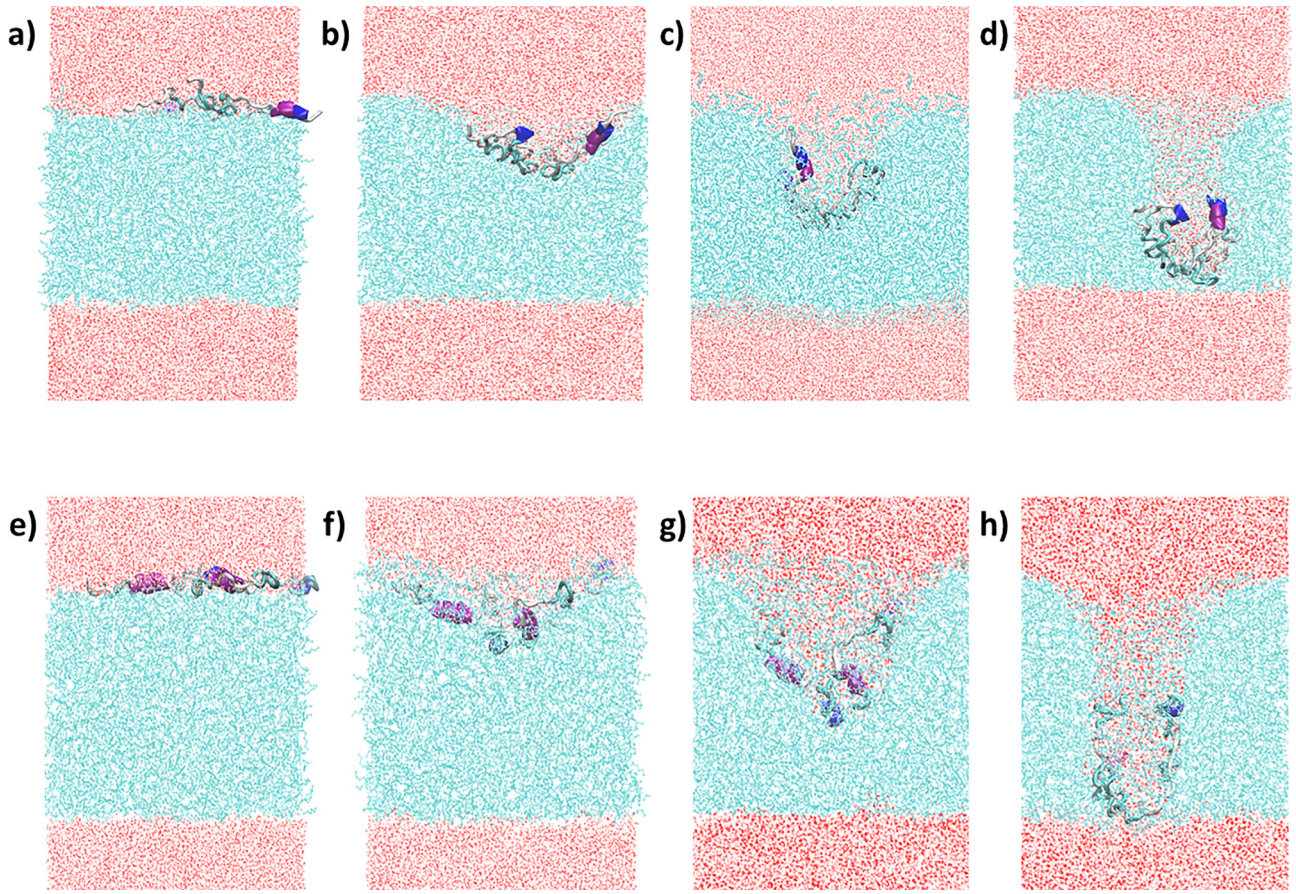

Fig. 5 US simulation snapshots of the translocation pathway of the four pHD24 peptides through the hexane–water interface at (a)–(d) pH 4 and (e)–(h) pH 7 in the AMBER force field. The periodic boundary condition is applied for the water molecules in the $-Z$ direction to clearly represent the image.

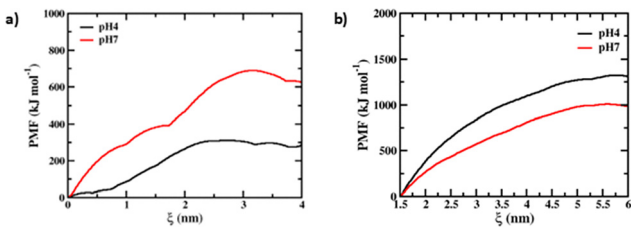

Fig. 6 PMF profile corresponds to the translocation of the four pHD24 peptides through the (a) octanol–water interface and (b) hexane–water interface at pH 4 (black) and pH 7 (red) in the AMBER force field.

protein indicated the importance of water permeation during peptide transport.

In the next section, we discuss the aggregation and translocation of the four pHD24 peptides through the heterogeneous lipid bilayer.

3.5. pHD24 aggregation and translocation through the heterogeneous membrane

In this section, we discuss the aggregation tendency and translocation of the four pHD24 peptides across the hydrophilic–hydrophobic interface of a heterogeneous lipid bilayer, consisting of POPC, POPS, and cholesterol lipids, at both pH 4 and 7.

Table 6 The hydrogen-bond lifetime (HBL) and diffusion coefficient (D_c) were computed for confined water during the translocation of peptides at pH 4 and 7 in the AMBER force field

Systems	pH	HBL (ps)	D_c (cm^2 s^{-1})
Octanol–water	4	2.98	2.58×10^{-5}
	7	2.59	2.76×10^{-5}
Hexane–water	4	3.09	2.67×10^{-5}
	7	2.82	3.26×10^{-5}

Similar to the octanol–water system, the pHD24 peptides tend to aggregate on the bilayer surface at pH 4. They had a more compact structure with an average R_g value of 2.16 ± 0.13 nm. They also formed a similar secondary structure on the membrane surface to the octanol–water interface. At pH 4, they exhibited a high tendency to form beta-sheets (2%) and beta-bridges (2%), which facilitated their aggregation. On the contrary, the peptides were randomly diffusing at pH 7 on the membrane surface, as they were more stabilized by the aqueous environment than by the membrane medium. Hence, the average R_g value was 3.44 ± 0.92 nm. In this case, the peptides tend to form an alpha-helix (1%) and a 3-helix (1%), which were absent at pH 4. The secondary structure plots of the pHD24 peptides at pH 4 and 7, when they are in the membrane interface, are provided in the SI (Fig. S8).

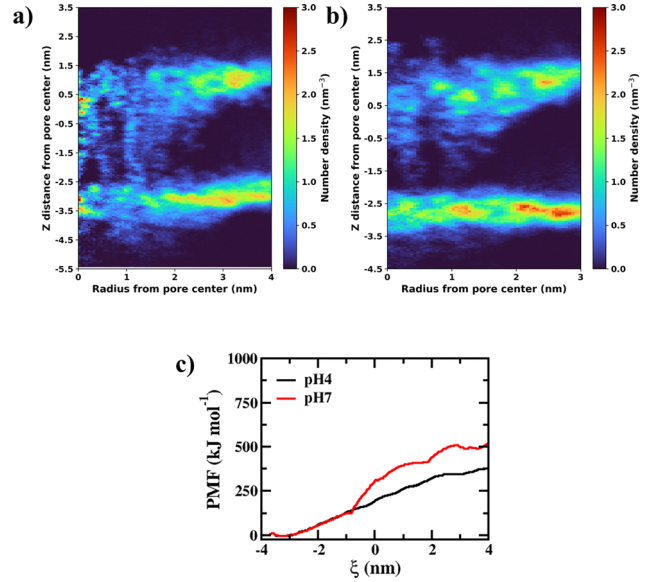

Fig. 7 Number densities (nm^{-3}) of the phosphate head groups computed during the translocation of the pHD24 peptides at (a) pH 4 and (b) pH 7. (c) PMF profile corresponds to the translocation of the four pHD24 peptides through the heterogeneous membrane at pH 4 (black) and pH 7 (red).

Next, we pulled all four pHD24 peptides through the hydrophobic core of the membrane at pH 4 and 7 to study the translocation pathways and computed the permeation barrier to cross the heterogeneous lipid bilayer. The snapshots corresponding to the translocation pathway of the peptides at both pH levels are given in Fig. S9.

The peptides were more compact at pH 4, and they translocated through the water channel along the lipid molecules, similar to those in the octanol–water interface system. Whereas the peptides were more dispersed on the membrane surface due to the high negative charge at pH 7. They faced more barriers to cross the membrane. At pH 7, out of four peptides, three peptides crossed the membrane, and the remaining peptide was anchored on the upper layer of the membrane. In this case, the peptides were translocated through a pore of a water channel, which was smaller than the pore created at pH 4. The pore size computed from the number density of phosphate head groups is given in Fig. 7a and b. The computed pore radii for pH 4 and 7 were 2.2 nm and 1.0 nm, respectively. The PMF profile computed during the permeation of the peptides through the membrane at pH 4 and 7 is shown in Fig. 7c.

From Fig. 7c, it is evident that the peptides face a low barrier at pH 4, with an energy cost of 381.7 kJ mol^{-1}. At pH 7, the peptides translocated with a barrier of 498.9 kJ mol^{-1}. The results are in good agreement with the peptide aggregation and translocation through the octanol–water interface systems.

4. Conclusions

To conclude, we found that the octanol–water interface was a better system for depicting the membrane–peptide interaction system for pHD peptides. At a low pH, the peptides were found to aggregate more due to the protonation state of histidine. The aggregation propensity of the peptides helped them to permeate smoothly at the lower pH through a water channel of bigger size. We found a similar trend when studying the heterogeneous lipid bilayer system. In the hexane–water system, the peptides were found to have less interactions with the solvent medium, which helped them to maintain their secondary structure. However, it increased their permeation barrier. The presence of the dispersed water molecules with a low density during peptide translocation through the hexane medium resulted in a long hydrogen bond lifetime. Therefore, the peptide–water and peptide-interface interactions were found to be important parameters for the permeation of the peptides.

Author contributions

Anjana V. Mathath: data curation, investigation, methodology, conceptualization, writing original draft, and reviewing. Samrat Sarkar: performed simulations and data curation. Debashree Chakraborty: conceptualization, methodology, investigation, writing original draft, reviewing, supervision, funding acquisition, project administration, resources.

Conflicts of interest

There are no conflicts to declare.

Data availability

The data supporting this article have been included within this article or its supplementary information (SI). Supplementary information includes hydrogen bond, interaction energy, secondary structure analysis data, and US snapshots of peptides translocation through the interfaces in the CHARMM force field. US snapshots of peptides translocation through membrane, pressure convergence, PMF convergence, R_g and RDF plots. See DOI: https://doi.org/10.1039/d5cp03690a.

Acknowledgements

Funding from the Science and Engineering Research Board, Department of Science and Technology, Government of India (WEA/2021/000004), is gratefully acknowledged. We also acknowledge the use of the PARAM UTKARSH HPC facility supported by the National Supercomputing Mission project, and we thank the Centre for Cyber Physical Systems (CCPS), National Institute of Technology Karnataka, Surathkal, for the financial support for the same. AVM acknowledges NITK for a fellowship. We would also like to thank the Department of Chemistry, NITK Surathkal, for their constant support.

References

1 Y. Nishimura, K. Takeda, R. Ezawa, J. Ishii, C. Ogino and A. Kondo, A display of pH-sensitive fusogenic GALA peptide

facilitates endosomal escape from a Bio-nanocapsule via an endocytic uptake pathway, *J. Nanobiotechnol.*, 2014, **12**, 11.
2 G. Moulay, C. Leborgne, A. J. Mason, C. Aisenbrey, A. Kichler and B. Bechinger, Histidine-rich designer peptides of the LAH4 family promote cell delivery of a multitude of cargo: Histidine-rich Cell Penetrating Peptide with Multiple Functionalities, *J. Pept. Sci.*, 2017, **23**, 320–328.
3 L. Yao, J. Daniels, D. Wijesinghe, O. A. Andreev and Y. K. Reshetnyak, pHLIP®-mediated delivery of PEGylated liposomes to cancer cells, *J. Controlled Release*, 2013, **167**, 228–237.
4 O. A. Andreev, D. M. Engelman and Y. K. Reshetnyak, pH-sensitive membrane peptides (pHLIPs) as a novel class of delivery agents, *Mol. Membr. Biol.*, 2010, **27**, 341–352.
5 M. An, D. Wijesinghe, O. A. Andreev, Y. K. Reshetnyak and D. M. Engelman, pH-(low)-insertion-peptide (pHLIP) translocation of membrane impermeable phalloidin toxin inhibits cancer cell proliferation, *Proc. Natl. Acad. Sci. U. S. A.*, 2010, **107**, 20246–20250.
6 S. Y. Kim, A. E. Pittman, E. Zapata-Mercado, G. M. King, W. C. Wimley and K. Hristova, Mechanism of Action of Peptides That Cause the pH-Triggered Macromolecular Poration of Lipid Bilayers, *J. Am. Chem. Soc.*, 2019, **141**, 6706–6718.
7 S. Y. Kim, A.-N. Bondar, W. C. Wimley and K. Hristova, pH-triggered pore-forming peptides with strong composition-dependent membrane selectivity, *Biophys. J.*, 2021, **120**, 618–630.
8 S. Guha, R. P. Ferrie, J. Ghimire, C. R. Ventura, E. Wu, L. Sun, S. Y. Kim, G. R. Wiedman, K. Hristova and W. C. Wimley, Applications and evolution of melittin, the quintessential membrane active peptide, *Biochem. Pharmacol.*, 2021, **193**, 114769.
9 E. Wu, A. Ellis, K. Bell, D. L. Moss, S. J. Landry, K. Hristova and W. C. Wimley, pH-Responsive Peptide Nanoparticles Deliver Macromolecules to Cells via Endosomal Membrane Nanoporation, *ACS Nano*, 2024, **18**, 33922–33936.
10 A. V. Mathath and D. Chakraborty, Effect of peptide hydrophilicity on membrane curvature and permeation, *J. Chem. Phys.*, 2024, **161**, 164105.
11 J. P. Nicolas, Molecular Dynamics Simulation of Surfactin Molecules at the Water-Hexane Interface, *Biophys. J.*, 2003, **85**, 1377–1391.
12 H. N. Dilip and D. Chakraborty, Hydrophilicity of the hydrophobic group: Effect of cosolvents and ions, *J. Mol. Liq.*, 2019, **280**, 389–398.
13 A. R. Zolghadr and S. Boroomand, Spontaneous assembly of HSP90 inhibitors at water/octanol interface: A molecular dynamics simulation study, *Chem. Phys. Lett.*, 2017, **669**, 130–136.
14 T. Fan, X. Yu, B. Shen and L. Sun, Peptide Self-Assembled Nanostructures for Drug Delivery Applications, *J. Nanomater.*, 2017, **2017**, 1–16.
15 E. Glukhov, M. Stark, L. L. Burrows and C. M. Deber, Basis for Selectivity of Cationic Antimicrobial Peptides for Bacterial Versus Mammalian Membranes, *J. Biol. Chem.*, 2005, **280**, 33960–33967.
16 A. Sepehri, L. PeBenito, A. Pino-Angeles and T. Lazaridis, What Makes a Good Pore Former: A Study of Synthetic Melittin Derivatives, *Biophys. J.*, 2020, **118**, 1901–1913.
17 S. Ciudad, E. Puig, T. Botzanowski, M. Meigooni, A. S. Arango, J. Do, M. Mayzel, M. Bayoumi, S. Chaignepain, G. Maglia, S. Cianferani, V. Orekhov, E. Tajkhorshid, B. Bardiaux and N. Carulla, Aβ(1-42) tetramer and octamer structures reveal edge conductivity pores as a mechanism for membrane damage, *Nat. Commun.*, 2020, **11**, 3014.
18 B. Bechinger, The SMART model: Soft Membranes Adapt and Respond, also Transiently, in the presence of antimicrobial peptides, *J. Pept. Sci.*, 2015, **21**, 346–355.
19 G. Wiedman, S. Y. Kim, E. Zapata-Mercado, W. C. Wimley and K. Hristova, pH-Triggered, Macromolecule-Sized Poration of Lipid Bilayers by Synthetically Evolved Peptides, *J. Am. Chem. Soc.*, 2017, **139**, 937–945.
20 J. Zhou, I. F. Thorpe, S. Izvekov and G. A. Voth, Coarse-Grained Peptide Modeling Using a Systematic Multiscale Approach, *Biophys. J.*, 2007, **92**, 4289–4303.
21 F. Grünewald, P. C. T. Souza, H. Abdizadeh, J. Barnoud, A. H. De Vries and S. J. Marrink, Titratable Martini model for constant pH simulations, *J. Chem. Phys.*, 2020, **153**, 024118.
22 N. V. Di Russo, D. A. Estrin, M. A. Martí and A. E. Roitberg, pH-Dependent Conformational Changes in Proteins and Their Effect on Experimental pKas: The Case of Nitrophorin 4, *PLoS Comput. Biol.*, 2012, **8**, e1002761.
23 A. Villa, A. E. Mark, G. A. A. Saracino, U. Cosentino, D. Pitea, G. Moro and M. Salmona, Conformational Polymorphism of the PrP106–126 Peptide in Different Environments: A Molecular Dynamics Study, *J. Phys. Chem. B*, 2006, **110**, 1423–1428.
24 J. J. Dwyer, A. G. Gittis, D. A. Karp, E. E. Lattman, D. S. Spencer, W. E. Stites and B. E. García-Moreno, High Apparent Dielectric Constants in the Interior of a Protein Reflect Water Penetration, *Biophys. J.*, 2000, **79**, 1610–1620.
25 W. E. Stites, A. G. Gittis, E. E. Lattman and D. Shortle, In a staphylococcal nuclease mutant the side-chain of a lysine replacing valine 66 is fully buried in the hydrophobic core, *J. Mol. Biol.*, 1991, **221**, 7–14.
26 M. Enciso, C. Schütte and L. Delle Site, Influence of pH and sequence in peptide aggregation via molecular simulation, *J. Chem. Phys.*, 2015, **143**, 243130.
27 J. S. Capes, P. J. Kiley and A. H. Windle, Investigating the Effect of pH on the Aggregation of Two Surfactant-Like Octapeptides, *Langmuir*, 2010, **26**, 5637–5644.
28 K. Lindorff-Larsen, S. Piana, K. Palmo, P. Maragakis, J. L. Klepeis, R. O. Dror and D. E. Shaw, Improved side-chain torsion potentials for the Amber ff99SB protein force field, *Proteins*, 2010, **78**, 1950–1958.
29 J. Huang, S. Rauscher, G. Nawrocki, T. Ran, M. Feig, B. L. De Groot, H. Grubmüller and A. D. MacKerell, CHARMM36m: an improved force field for folded and intrinsically disordered proteins, *Nat. Methods*, 2017, **14**, 71–73.
30 M. J. Abraham, T. Murtola, R. Schulz, S. Páll, J. C. Smith, B. Hess and E. Lindahl, GROMACS: High performance

molecular simulations through multi-level parallelism from laptops to supercomputers, *SoftwareX*, 2015, **1–2**, 19–25.
31 L. Martínez, R. Andrade, E. G. Birgin and J. M. Martínez, P Ackmol: A package for building initial configurations for molecular dynamics simulations, *J. Comput. Chem.*, 2009, **30**, 2157–2164.
32 J. L. F. Abascal and C. Vega, A general purpose model for the condensed phases of water: TIP4P/2005, *J. Chem. Phys.*, 2005, **123**, 234505.
33 M. D. Hanwell, D. E. Curtis, D. C. Lonie, T. Vandermeersch, E. Zurek and G. R. Hutchison, Avogadro: an advanced semantic chemical editor, visualization, and analysis platform, *J. Cheminf.*, 2012, **4**, 17.
34 H. J. C. Berendsen, J. P. M. Postma, W. F. Van Gunsteren, A. DiNola and J. R. Haak, Molecular dynamics with coupling to an external bath, *J. Chem. Phys.*, 1984, **81**, 3684–3690.
35 U. Essmann, L. Perera, M. L. Berkowitz, T. Darden, H. Lee and L. G. Pedersen, A smooth particle mesh Ewald method, *J. Chem. Phys.*, 1995, **103**, 8577–8593.
36 B. Hess, H. Bekker, H. J. C. Berendsen and J. G. E. M. Fraaije, LINCS: A linear constraint solver for molecular simulations, *J. Comput. Chem.*, 1997, **18**, 1463–1472.
37 W. Humphrey, A. Dalke and K. Schulten, VMD: Visual molecular dynamics, *J. Mol. Graphics*, 1996, **14**, 33–38.
38 E. L. Wu, X. Cheng, S. Jo, H. Rui, K. C. Song, E. M. Dávila-Contreras, Y. Qi, J. Lee, V. Monje-Galvan, R. M. Venable, J. B. Klauda and W. Im, CHARMM-GUI *Membrane Builder* toward realistic biological membrane simulations, *J. Comput. Chem.*, 2014, **35**, 1997–2004.
39 P. Bauer, B. Hess and E. Lindahl, *GROMACS 2022.2*, Source Code, Zenodo, 2022, DOI: 10.5281/ZENODO.6637571.
40 J. B. Klauda, R. M. Venable, J. A. Freites, J. W. O'Connor, D. J. Tobias, C. Mondragon-Ramirez, I. Vorobyov, A. D. MacKerell and R. W. Pastor, Update of the CHARMM All-Atom Additive Force Field for Lipids: Validation on Six Lipid Types, *J. Phys. Chem. B*, 2010, **114**, 7830–7843.
41 J. Huang, S. Rauscher, G. Nawrocki, T. Ran, M. Feig, B. L. De Groot, H. Grubmüller and A. D. MacKerell, CHARMM36m: an improved force field for folded and intrinsically disordered proteins, *Nat. Methods*, 2017, **14**, 71–73.
42 W. L. Jorgensen, J. Chandrasekhar, J. D. Madura, R. W. Impey and M. L. Klein, Comparison of simple potential functions for simulating liquid water, *J. Chem. Phys.*, 1983, **79**, 926–935.
43 S. Nosé and M. L. Klein, Constant pressure molecular dynamics for molecular systems, *Mol. Phys.*, 1983, **50**, 1055–1076.
44 J. Kästner, Umbrella sampling: Umbrella sampling, *WIREs Comput. Mol. Sci.*, 2011, **1**, 932–942.
45 S. Kumar, J. M. Rosenberg, D. Bouzida, R. H. Swendsen and P. A. Kollman, THE weighted histogram analysis method for free-energy calculations on biomolecules. I. The method, *J. Comput. Chem.*, 1992, **13**, 1011–1021.
46 O. Singh and D. Chakraborty, Preferential binding affinity of ions and their effect on structure and dynamics of water near antimicrobial peptide, *J. Mol. Liq.*, 2021, **344**, 117789.
47 D. Chakraborty and A. Chandra, Voids and necks in liquid ammonia and their roles in diffusion of ions of varying size, *J. Comput. Chem.*, 2012, **33**, 843–852.
48 A. V. Mathath, B. K. Das and D. Chakraborty, Designing Reaction Coordinate for Ion-Induced Pore-Assisted Mechanism of Halide Ions Permeation through Lipid Bilayer by Umbrella Sampling, *J. Chem. Inf. Model.*, 2023, **63**, 7778–7790.
49 J. H. Simpson and H. Y. Carr, Diffusion and Nuclear Spin Relaxation in Water, *Phys. Rev.*, 1958, **111**, 1201–1202.
50 D. V. Zlenko, Computing the self-diffusion coefficient for TIP4P water, *Biophysics*, 2012, **57**, 127–132.
51 J. T. Su, P. B. Duncan, A. Momaya, A. Jutila and D. Needham, The effect of hydrogen bonding on the diffusion of water in n-alkanes and n-alcohols measured with a novel single microdroplet method, *J. Chem. Phys.*, 2010, **132**, 044506.

